25.11% efficiency silicon heterojunction solar cell with low deposition rate intrinsic amorphous silicon buffer layers

Xiaoning Ru [a], Minghao Qu [a,b,**], Jianqiang Wang [b], Tianyu Ruan [b], Miao Yang [a], Fuguo Peng [a], Wei Long [a], Kun Zheng [b], Hui Yan [b], Xixiang Xu [a,*]

[a] Hanergy Thin Film Power Group, Chengdu R&D Center, Chengdu, Sichuan, 610200, China
[b] Beijing University of Technology, Beijing, 100124, China

ABSTRACT

Here we report a certified efficiency of up to 25.11% for silicon heterojunction (SHJ) solar cells on a full size n-type M2 monocrystalline-silicon (c-Si) wafer (total area, 244.5 cm^2). An ultra-thin intrinsic a-Si:H buffer layer was introduced on the c-Si wafer surface using a 13.56 MHz home-made RF-PECVD with low deposition rate showing superior surface passivation. The ultra-thin i-a-Si:H film with both higher microstructure factor (R*) and H content evidently increases the SHJ solar cell open-circuit voltage (V_{OC}) by 2 mV, and moreover, short-circuit current (I_{SC}) and fill factor (*FF*) are also notably improved, resulting in a 0.52% absolute cell efficiency enhancement, in which *FF* is the main cause. In order to explore high conversion efficiency SHJ solar cells, both home-made RF-PECVD and commercial VHF-PECVD (40.68 MHz) are employed for deposition of the i-a-Si:H passivation layer. As a result, the efficiency of RF-PECVD-prepared SHJ cell is 0.21% higher than that of VHF-PECVD-prepared, mainly driven by V_{OC} and I_{SC} boost. This work offers a useful tool for fabrication of high performance SHJ solar cells which could be employed in mass production.

1. Introduction

In recent years, silicon heterojunction (SHJ) solar cell technology has demonstrated great potential in both exploring high conversion efficiency and upscaling towards mass production, owing to its bifacial capability, low operating temperature coefficient, and relatively straightforward manufacturing process [1–3]. Multiple SHJ efficiency milestones have been reported worldwide [4–10], accomplished through various materials, methods, and/or tools. For instance, Panasonic announced a total area (t.a., 101.8 cm^2) conversion efficiency of 24.7%, using plasma enhanced chemical vapor deposition (PECVD), reactive plasma deposition (RPD), and screen-printed silver electrodes [4]. In contrast, Kaneka later set the record (t.a., 239.0 cm^2) efficiency of 24.5% and aperture area (151.9 cm^2) efficiency of 25.1% with plasma enhanced chemical vapor deposition (PECVD), physical vapor deposition (PVD), and electroplated copper grid fingers [5]. Previously, we also reported a 24.85% (t.a., 244.5 cm^2) efficiency based on PECVD, PVD, and screen-print process [11]. In addition to these leading efficiencies for the front-rear contacted SHJ solar cells, the formation of

interdigitated back contact (IBC) structure enables extra efficiency benefits and makes SHJ + IBC (HBC) the most efficient device among the crystalline-silicon-based photovoltaics technologies [12–16].

A high V_{OC} for a SHJ solar cell is required to achieve a high efficiency, which relies on excellent passivation of the c-Si surface that is mainly dominated by hydrogenation of silicon dangling bonds and reduction of interfacial defect density with intrinsic amorphous silicon (i-a-Si:H) layers [17,18]. The properties of the i-a-Si:H layers, e.g., deposited by PECVD, could be largely influenced by a number of factors, typically including deposition power, pressure, temperature [19,20], hydrogen dilution [21,22], *in-situ* hydrogen plasma treatment (HPT) [23–25], thermal annealing [26–28], bi-layers [29,45,46], etc. Furthermore, intrinsic silicon-based alloy alternatives like amorphous silicon-oxide (a-SiO$_x$:H) [30] and amorphous silicon-carbide (a-SiC$_x$:H) [31] are also applicable for improving c-Si surface passivation. In most cases, a combination of several turning knobs may be needed. Liu et al. reported that a less dense i-a-Si:H layer was beneficial to V_{OC} if it is capped with a dense a-Si:H layer [32]. Zhang et al. showed that i-a-Si:H bi-layer with a porous interfacial layer improved the minority carrier

---

* Corresponding author.
** Corresponding author.
  E-mail addresses: qqkitfk@emails.bjut.edu.cn (M. Qu), xixiangxu@comcast.net (X. Xu).

(a) RF-PECVD-prepared intrinsic layer with i1 buffer layer

TCO
n-a-Si:H/μc-SiOx:H
i-a-Si:H
i₁ a-Si:H buffer

(n) c-Si

i₁ a-Si:H buffer
i-a-Si:H
p-a-Si:H
TCO

(b) RF-PECVD-prepared intrinsic layer

TCO
n-a-Si:H/μc-SiOx:H
i-a-Si:H

(n) c-Si

i-a-Si:H
p-a-Si:H
TCO

(c) VHF-PECVD-prepared intrinsic layer

TCO
n-μc-SiOx:H
i-a-Si:H

(n) c-Si

i-a-Si:H
p-a-Si:H
TCO
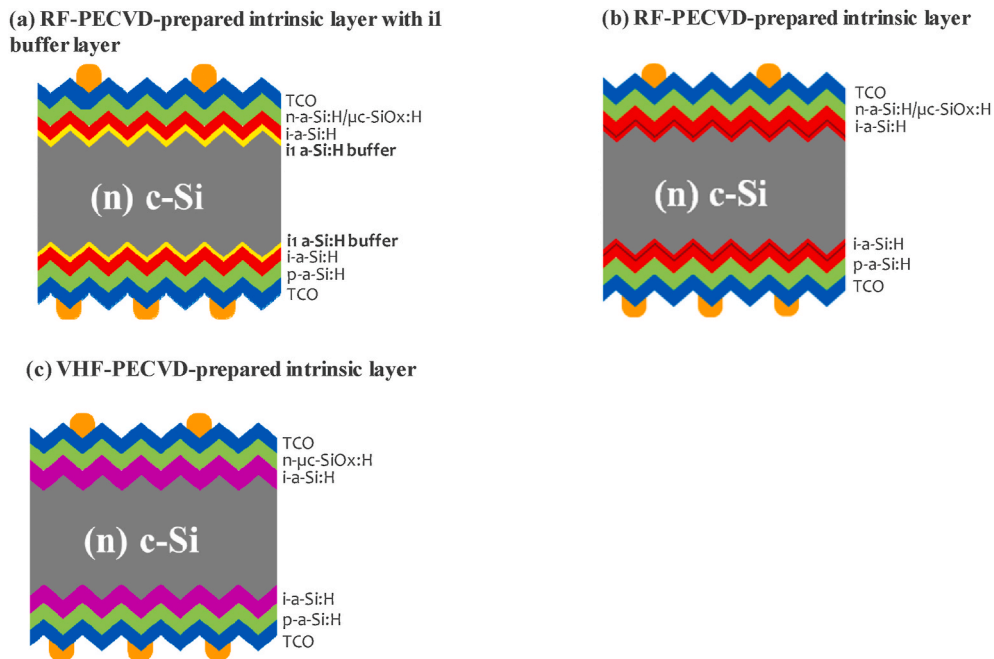
Fig. 1. Schematic illustration of the SHJ solar cell structure: (a) RF-PECVD-prepared intrinsic layer with i_1 buffer layer, (b) RF-PECVD-prepared normal intrinsic layer, (c) VHF-PECVD-prepared intrinsic layer.

Table 1
Summary of main pecvd process parameters.

Layer	Thickness (nm)	Temperature (°C)	Pressure (mbar)	Power Density (mW/cm²)
I1-a-Si:H (RF)	0.5–1	220	0.7	15.8
i-a-Si:H (RF)	7	220	0.8	21
i-a-Si:H (VHF)	8	200	0.5	30.5
n-μc-SiO$_x$:H (VHF)	20	200	2	180
p-a-Si:H (VHF)	8	200	0.5	35

lifetime [33]. Similarly, Sai's group also demonstrated that i-a-Si:H bilayer with a porous interfacial layer with high hydrogen content could substantially improve the implied V_{OC} and pseudo fill factor (pFF) of SHJ solar cells [29].

Very-high-frequency (VHF-) excited PECVD is commonly used [21, 34], as in the above scenarios, to grow i-a-Si:H at a relatively high deposition rate (>8 Å/s) with elevated power density, to avoid epitaxial growth near the a-Si:H/c-Si interface. However, VHF-PECVD prepared a-Si:H films often exhibit high bulk defect density and non-uniformity [36], which may lead to efficiency losses. On the other hand, PECVD powered by radio-frequency (RF-) excitation is expected to improve the film quality due to a lower deposition rate (~2 Å/s). However, the risk of plasma induced defects and epitaxial growth at the interface becomes more prominent [21,28,37]. Therefore, the trade-off between interfacial passivation and bulk quality of i-a-Si:H layer makes it challenging for RF-PECVD-based process development.

In this work, we introduce a low deposition rate, approximately 2 Å/s, i-a-Si:H (i_1) buffer layer grown prior to the bulk i-a-Si:H layer, both deposited with RF-PECVD, as shown in Fig. 1a, to improve c-Si surface passivation and thus the efficiency of SHJ solar cell. The optical and structural properties of i_1 buffer layer are studied by spectral transmittance and Fourier transform infrared (FTIR) spectroscopy. The surface passivation quality of the i_1+i-a-Si:H stack is evaluated with passivated samples. SHJ solar cells with i-a-Si:H layers deposited by RF- and VHF-PECVD are fabricated and compared. As a result, the insertion of i_1 buffer layer substantially improved the cell performance and we report a new total area efficiency of 25.11% on an M2 c-Si wafer.

2. Experimental details

In this study, deposition of the i_1 and i-a-Si:H films was conducted in a home-made parallel plate RF-PECVD (13.56 MHz) reactor. Optical transmittance of a-Si:H deposited on glass substrate was characterized by a PerkinElmer Lambda 950 spectrometer. FTIR responses were captured by a Nicolet IS-10 spectrometer with a-Si:H films (~15 nm) deposited on a 500 μm thick polished (100) oriented c-Si (1000 Ω cm) substrates. Thicknesses of a-Si:H films were confirmed by a Syscos spectroscopic ellipsometer. Passivated samples were made in a symmetrical structure: covered by identical intrinsic and doped layers, either with or without i_1 buffer (see Fig. 1a and b), on both surfaces of the double side textured and cleaned c-Si wafer. The effective minority carrier lifetime (τ_{eff}) was measured by a Sinton WCT-120 flash tester in transient mode. Two Ideal Energy VHF-PECVD (40.68 MHz) systems were used to deposit the reference i-a-Si:H, p-type a-Si:H, and n-type μc-SiO$_x$:H layers during the cell fabrication. The main PECVD deposition parameters are listed in Table 1.

All SHJ solar cells were bifacial, fabricated on LONGi n-type M2 CZ c-Si wafers, with resistivity of 1–5 Ω cm, thickness of 150 μm, in (100) orientation. Intrinsic a-Si:H layers, as described in Table 1, were deposited with RF- or VHF-PECVD, capped by the same doped layers (see Fig. 1a and c). TCO layers were formed by a home-made PVD tool using 90:10 indium-tin-oxide (ITO) material sputtered from a rotary target. Silver grid electrodes were screen printed followed by a 190 °C curing for 30 min. Current–voltage (I–V) characteristics of SHJ solar cells were taken by a Vision VS-6821S I-V tester under standard test
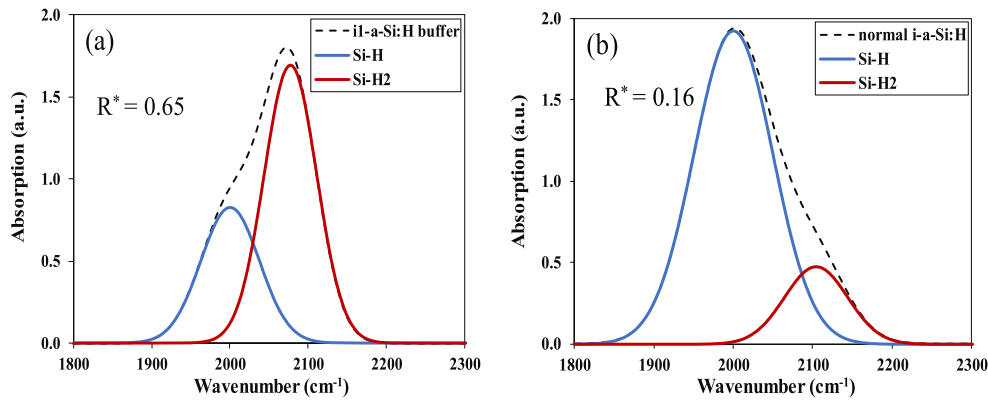
Fig. 2. FTIR spectra for i_1 buffer and normal i-a-Si:H layers deposited by RF-PECVD, fitted with two Gaussian-distributed absorption peaks centered at wavenumbers of 2000 cm^{-1} and 2100 cm^{-1}, representing monohydride (Si-H) bond and dihydrides (Si-H$_2$) bond stretching modes, respectively.
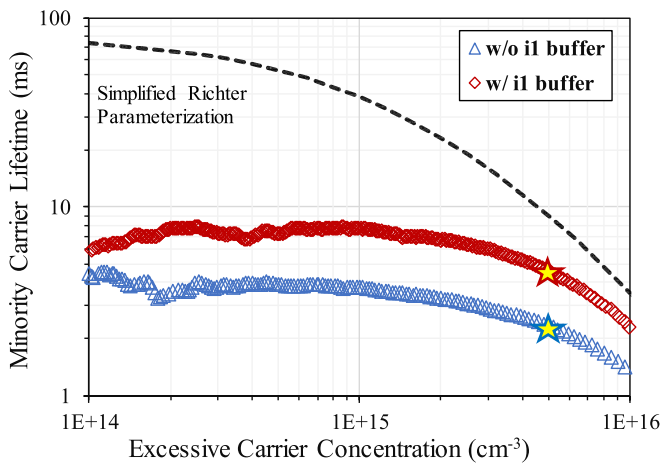

Fig. 3. The τ_{eff} of the passivated samples fabricated with and without ultra-thin i_1 buffer layer, where τ_{eff} is obtained at a carrier injection level of 5×10^{15} cm^{-3}. The dashed line is plotted according to simplified Richter parameterization [43].

condition (AM 1.5G, 1000 W/m^2, 25 °C). All cells were illuminated from the n-side and the conversion efficiency was calculated on the total area of 244.5 cm^2. External quantum efficiency (EQE) and reflectance spectra of SHJ solar cells were measured on the entire front surface including the grid-shaded area with Bentham PVE300-IVT system over the wavelengths ranging from 300 nm to 1170 nm.

3. Results and discussion

The FTIR spectra of RF-PECVD deposited 15-nm-thick i_1 buffer and normal i-a-Si:H layers on polished c-Si substrates are shown in Fig. 2, fitted with two Gaussian-distributed absorption peaks centered at wavenumbers of 2000 cm^{-1} and 2100 cm^{-1}, representing monohydride (Si-H) bond and dihydrides (Si-H$_2$) bond stretching modes, respectively [38–40]. The relative intensities of Si-H and Si-H$_2$ absorption for i_1 buffer (see Fig. 2a) and normal i-a-Si:H (see Fig. 2b) layers are significantly different. We observed a greater contribution of Si-H$_2$ mode in the overall absorption for i_1 buffer layer, implying a higher void density and more disordered hydrogen incorporation within the film [41]. The microstructure factor R*, defined as R* = $I_{Si-H2}/(I_{Si-H2}+I_{Si-H})$, where I_{Si-H2} and I_{Si-H} are peak intensities, is 0.65 for i_1 buffer layer and 0.16 for normal i-a-Si:H layer. Hydrogen content calculation (CH) is carried out as introduced by Langford reported [47], which is related to the stretching-mode absorption via CH = A$_{2000}$I$_{2000}$+A$_{2090}$I$_{2090}$ =

A$_{2000}$∫(α/ω)dω+A$_{2090}$∫(α/ω)dω, where, α is the absorption coefficient, ω is the frequency in cm^{-1}, A is the proportionality constant, which are A$_{2000}$ = 9.0 × 10^{19} cm^{-2}, and A$_{2090}$ = 2.2 × 10^{22} cm^{-2}, respectively. The sum of Si-H and Si-H$_2$ peak integrals gives a 25.8% hydrogen content for i_1 buffer layer and 15.8% for normal a-Si:H layer [41].

In general, high quality i-a-Si:H material with lower void density (lower R*) is beneficial to the performance of SHJ solar cells [48,49]. However, during RF-PECVD deposition, the epitaxial growth at the a-Si: H/c-Si interface may have a detrimental impact on the surface passivation [35]. In spite of the defective nature, the hydrogen-rich i_1 buffer layer is still expected to improve the passivation by forming an abrupt a-Si:H/c-Si interface [42], as long as the thickness of such layer is controlled in a range of 0.5-1.0 nm. We found that a 0.5–1.0 nm ultra-thin i_1 buffer layer underneath the bulk i-a-Si:H layer could play a pivotal role in the surface passivation. Fig. 3 gives the τ_{eff} of the passivated samples fabricated with and without ultra-thin i_1 buffer layer, where τ_{eff} is obtained at a carrier injection level of 5×10^{15} cm^{-3}. The total i-a-Si:H film thicknesses remained the same. After inserting the i_1 buffer layer, τ_{eff} exhibited a substantial increase from 2.3 ms to 4.5 ms, which implied that the hydrogen-rich yet defective i_1 buffer layer can effectively improve surface passivation. It is confirmed that the iV$_{OC}$ of the two passivated samples in Fig. 1 (see Fig. 1a and b) were 749.8 mV and 745.7 mV, respectively, where a 4.1 mV gap means that the i1+ i-a-Si:H film stack process has room for further optimization. It could be attributed to effectively saturated silicon dangling bonds and probably minimized interfacial epitaxial growth under low deposition rate conditions during the RF-PECVD process. Furthermore, it may be ascribed to increased band offsets, thus increased barrier for charge transport [50]. Further research for good surface passivation with hydrogen-rich a-Si:H is ongoing in our project.

The effect of ultra-thin i_1 a-Si:H buffer layer on SHJ solar cell performances were verified by two groups of cells, four cells per group, fabricated with and without i_1 buffer layer on both n and p sides (see Fig. 1a and b). Except for the abovementioned different interfacial ultra-thin i-a-Si:H layer (less than 1 nm) configuration, process conditions for the remaining layers remain the same, where a 6 nm n-type a-Si:H layer, a 8 nm p-type a-Si:H layer, a 70 nm multi-layer-stack ITO layer both for front and rear side, and a five-busbar Ag screen-printed front grid were applied for two groups' cell fabrication. As a proof of concept experiment on pilot line, all non-intrinsic a-Si:H components were designed suitably for mass production without further tuning. Both groups of SHJ cells adopted the multi-i-layer structure designed for cell efficiency enhancement. The i_1 buffer layers were prepared at a low deposition rate of 2.3 Å/s. Bulk i-a-Si:H layers were deposited by RF-PECVD in both cases. As shown in Fig. 4 (Batch A), the i_1 buffer layer gives rise to a 2-mV benefit in V$_{OC}$, which is consistent with the improved surface passivation suggested by the τ_{eff} measurements. In addition, increased
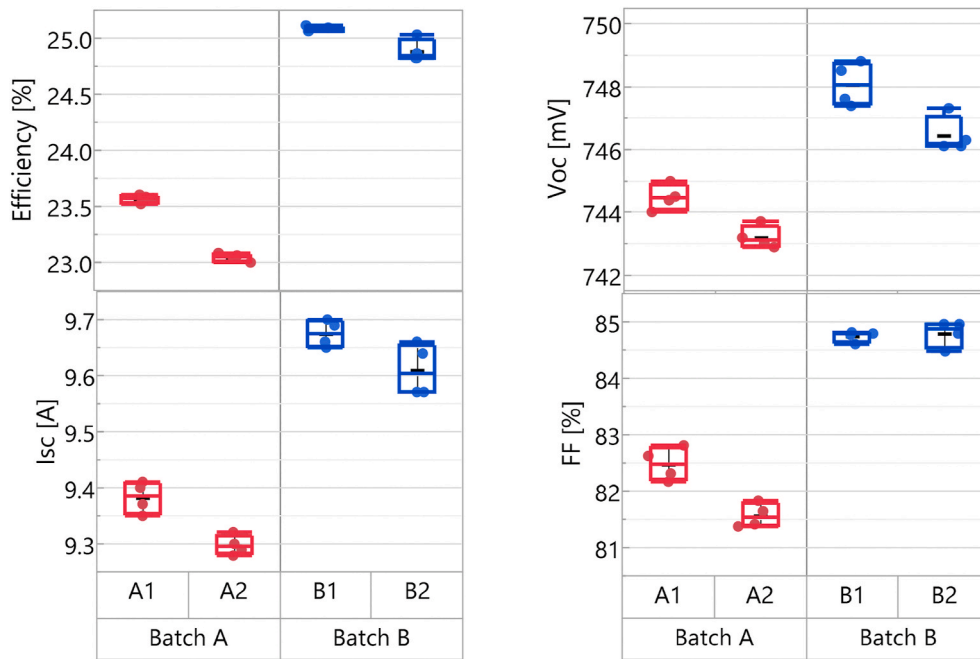
Fig. 4. The illuminated I-V parameters of two batches SHJ solar cells on M2 wafers, Batch A: two groups cells from RF-PECVD, A1: with ultra-thin i1 buffer layer, A2: without ultra-thin i1 buffer layer and Batch B: two groups cells with RF-PECVD i-a-Si:H layers (B1) and VHF-PECVD i-a-Si:H layers (B2).
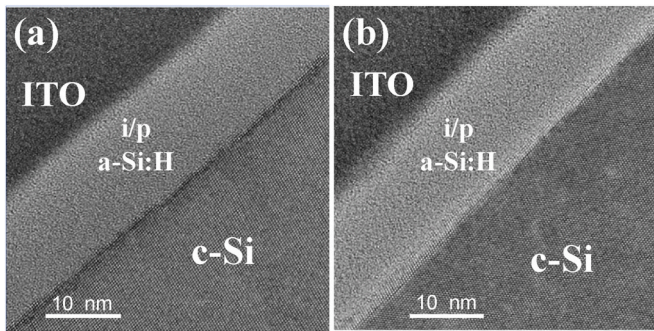

Fig. 5. Cross-sectional TEM images taken at the a-Si:H/c-Si interfaces with (a) RF-PECVD and (b) VHF-PECVD deposited i-a-Si:H layers.

Fig. 6. EQE and reflectance (refl.) spectra of SHJ solar cells with RF- and VHF-PECVD deposited i-a-Si:H layers. The inset shows the transmittance spectra acquired with 100-nm-thick i-a-Si:H layers on glass substrates and transmittance spectra of reference bare glass substrate.

I_{SC} and *FF* are also obtained, which may be related to the enhanced optical transmittance and carrier transportation, respectively. As a result, it ends up with an improvement of 0.52% in conversion efficiency.

Prior to the current work, our SHJ solar cells of champion efficiency were all processed by VHF-PECVD [44]. Fig. 5 shows the cross-sectional TEM images taken at the a-Si:H/c-Si interfaces of the best-performing cells with RF-PECVD (Fig. 5a) and VHF-PECVD (Fig. 5b) deposited i-a-Si:H layers. In both cases, we observed atomically sharp interfaces without traces of epitaxy. During VHF-PECVD reactions, higher deposition rate could prevent epitaxial growth due to abundant silyl radicals which can facilitate transition from crystalline to amorphous phase [19, 35]. In our study, deposition rate of VHF-PECVD was 7.8 Å/s, which is closed to that reported by S. Kim et al., 8.3 Å/s [19]. By employing a 3-fold lower deposition rate (2.3 Å/s) i_1 buffer layer, RF-PECVD is also capable of forming good surface passivation and V_{OC} is not affected.

Fig. 6 shows EQE and reflectance (refl.) spectra of SHJ solar cells with RF- and VHF-PECVD deposited i-a-Si:H layers (see Fig. 1a and c). When RF-PECVD i-a-Si:H layer used, EQE enhancement in the region of 300-650 nm but no reflectance difference is observed in the whole region, suggesting that a change in reflection is not the source of the gain. Also indicated by the inset of Fig. 6 is better optical transmittance of RF-
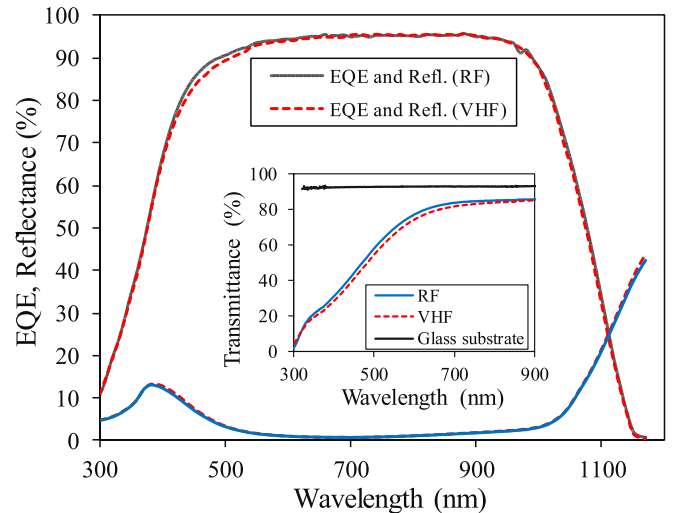
PECVD i-a-Si:H film deposited on glass substrate, which could be responsible for the I_{SC} gain in the above region. It turns out that the optical bandgap of RF-PECVD i-a-Si:H layers is higher, probably due to the elevated hydrogen content within the i_1 buffer layer. Thus, it is a promising candidate to further reduce the parasitic absorption and to enhance the carrier collection in the SHJ solar cell.

The I-V characteristics of the SHJ solar cells with RF- and VHF-PECVD processed i-a-Si:H layers are compared in Fig. 4 (Batch B), four cells per group. To evaluate the two PECVD processes, as well as to further explore the efficiency potential of SHJ solar cells, RF- and VHF-PECVD based i-a-Si:H layers were further integrated with other optimization methods, including fine tuning of the stack layer structure, layer thickness distribution and total film thickness, to reach their best cell performing (see Fig. 1a and c). Compared to Batch A, two major
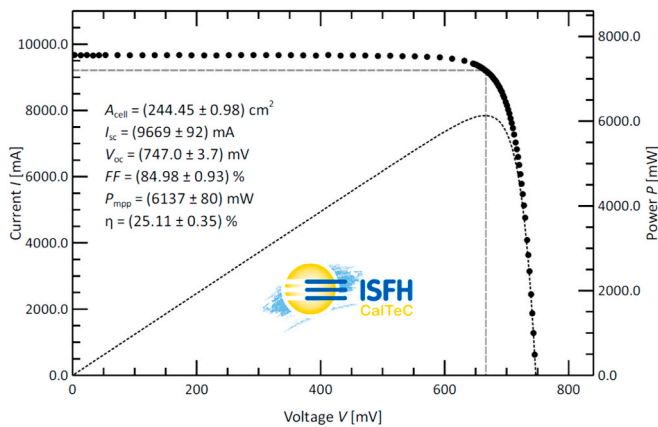
Fig. 7. I-V characteristics of a 25.11% efficiency SHJ solar cell on a total area of 244.5 cm², certified by ISFH.

components of a 20 nm n-type μc-SiOx:H layer and a 12 busbar Ag screen-printed front grid, combined with an addition antireflection coating on top of the cell, were specifically designed to pursue higher cell efficiency, while all other components process remained the same. From Fig. 4 (Batch B), RF-PECVD cell exhibits even higher V_{OC}, compared with VHF-PECVD. The I_{SC} difference is in good agreement with the shift in EQE spectra as shown in Fig. 6. In-house measurements show that the efficiency of RF-PECVD cell is higher by 0.21%, mainly driven by Isc and Voc boost.

The same optimization strategies (RF-PECVD based) were employed and verified in SHJ pilot line. Combined with other fine tuning steps, including wafer cleaning, environment control, and operation standardization, eventually a total area efficiency of 25.11% for SHJ solar cell was achieved and certified by the Institute for Solar Energy Research in Hamelin (ISFH), with V_{OC} = 747.0 mV, I_{SC} = 9.669 A, and FF = 84.98%, on a total area of 244.5 cm² (see Fig. 7). Noticeably, for the contacting of our multi-busbar cells, very thin contact bars were used, which has a thin and elastic contact plate inside. Wherein, each bar has 30 contact points, equally distributed over the busbar.

4. Conclusions

In summary, a 0.5–1 nm i₁ a-Si:H buffer layer deposited by RF-PECVD with high hydrogen content and large microstructure factor (R*) was introduced, which improved the c-Si surface passivation effectively. The results showed that no epitaxial growth was observed at the a-Si:H/c-Si interface when an i-a-Si:H buffer layer was grown with low deposition rate using RF-PECVD. It was also shown that one could get generally equivalent surface passivation with either RF- or VHF-PECVD tools. Incorporation of the RF-PECVD processed i₁+i-a-Si:H film stack resulted in a 0.21% efficiency advantage compared with VHF-PECVD based cells, mainly driven by Isc and Voc improvement. The efficiency of 25.11% certified by ISFH was obtained on a total area of 244.5 cm².

The results suggest that RF-PECVD deposited low-deposition-rate i-a-Si:H is a good material for buffer layers to boost cell performance. Further investigation is also needed to better understand the FF improvement in the presence of i₁-a-Si:H layers prepared by RF-PECVD.

Declaration of competing interest

The authors declare that they have no known competing financial interests or personal relationships that could have appeared to influence the work reported in this paper.

CRediT authorship contribution statement

Xiaoning Ru: Writing - original draft. **Minghao Qu:** Supervision. **Jianqiang Wang:** Conceptualization. **Tianyu Ruan:** Formal analysis. **Miao Yang:** Methodology. **Fuguo Peng:** Validation. **Wei Long:** Writing - review & editing. **Kun Zheng:** Resources. **Hui Yan:** Funding acquisition. **Xixiang Xu:** Supervision.

Acknowledgments

References

[1] S. De Wolf, A. Descœudres, Z.C. Holman, C. Ballif, High-efficiency silicon heterojunction solar cells: a review, Greenpeace 2 (2012) 7–24, https://doi.org/10.1515/green-2011-0018.

[2] J. Haschke, O. Dupré, M. Boccard, C. Ballif, Silicon heterojunction solar cells: recent technological development and practical aspects - from lab to industry, Sol. Energy Mater. Sol. Cells 187 (2018) 140–153, https://doi.org/10.1016/j.solmat.2018.07.018.

[3] C. Ballif, M. Boccard, A. Descœudres, C. Allebé, A. Faes, O. Dupré, J. Haschke, P.-J. Ribeyron, M. Despeisse, Solving all bottlenecks for silicon heterojunction technology, Photovoltaics International 42 (2019) 85–97.

[4] M. Taguchi, A. Yano, S. Tohoda, K. Matsuyama, Y. Nakamura, T. Nishiwaki, K. Fujita, E. Maruyama, 24.7% record efficiency hit solar cell on thin silicon wafer, IEEE J. Photovoltaics 4 (2014) 96–99, https://doi.org/10.1109/jphotov.2013.2282737.

[5] D. Adachi, J.L. Hernández, K. Yamamoto, Impact of carrier recombination on fill factor for large area heterojunction crystalline silicon solar cell with 25.1% efficiency, Appl. Phys. Lett. 107 (2015), https://doi.org/10.1063/1.4937224, 233506.

[6] G. Condorelli, W. Favre, A. Battaglia, P. Rotoli, A. Canino, M. Sciuto, A. Ragonesi, A. Danel, D. Munoz, C. Roux, J.F. Lerat, F. Medlege, V. Barth, L. Sicot, P. J. Ribeyron, C. Gerardi, High efficiency hetero-junction: from pilot line to industrial production, in: Proceedings of the 7th IEEE World Conference on Photovoltaic Energy Conversion, WCPEC 2018, Waikoloa Village, HI, USA, 2018, pp. 1970–1973, https://doi.org/10.1109/PVSC.2018.8548197.

[7] A. Richter, V. Smirnov, A. Lambertz, K. Nomoto, K. Welter, K. Ding, Versatility of doped nanocrystalline silicon oxide for applications in silicon thin-film and heterojunction solar cells, Sol. Energy Mater. Sol. Cells 174 (2018) 196–201, https://doi.org/10.1016/j.solmat.2017.08.035.

[8] J. Zhao, M. Konig, Y. Yao, Y. Wang, R. Zhou, T. Xie, H. Deng, 24% silicon heterojunction solar cells on meyer burger's on mass production tools and how wafer material impacts cell parameters, in: Proceedings of the 7th IEEE World Conference on Photovoltaic Energy Conversion, WCPEC, 2018, pp. 1514–1519, https://doi.org/10.1109/PVSC.2018.8547908, 2018.

[9] A.N. Fioretti, M. Boccard, R. Monnard, C. Ballif, Low-temperature p-type microcrystalline silicon as carrier selective contact for silicon heterojunction solar cells, IEEE J. Photovoltaics 9 (2019) 1158–1165, https://doi.org/10.1109/JPHOTOV.2019.2917550.

[10] Z. Wu, L. Zhang, R. Chen, W. Liu, Z. Li, F. Meng, Z. Liu, Improved amorphous/crystalline silicon interface passivation for silicon heterojunction solar cells by hot-wire atomic hydrogen during doped a-si:H deposition, Appl. Surf. Sci. 475 (2019) 504–509, https://doi.org/10.1016/j.apsusc.2018.12.239.

[11] Hanergy sets new efficiency record for heterojunction cell. https://www.pv-magazine/2019/08/08/hanergy-sets-new-efficiency-record-for-heterojunction-module/.

[12] K. Masuko, M. Shigematsu, T. Hashiguchi, D. Fujishima, M. Kai, N. Yoshimura, T. Yamaguchi, Y. Ichihashi, T. Mishima, N. Matsubara, T. Yamanishi, T. Takahama, M. Taguchi, E. Maruyama, S. Okamoto, Achievement of more than 25% conversion efficiency with crystalline silicon heterojunction solar cell, IEEE J. Photovoltaics 4 (2014) 1433–1435, https://doi.org/10.1109/jphotov.2014.2352151.

[13] K. Yoshikawa, W. Yoshida, T. Irie, H. Kawasaki, K. Konishi, H. Ishibashi, T. Asatani, D. Adachi, M. Kanematsu, H. Uzu, K. Yamamoto, Exceeding conversion efficiency of 26% by heterojunction interdigitated back contact solar cell with thin film si technology, Sol. Energy Mater. Sol. Cells 173 (2017) 37–42, https://doi.org/10.1016/j.solmat.2017.06.024.

[14] J. Nakamura, N. Asano, T. Hieda, C. Okamoto, H. Katayama, K. Nakamura, Development of heterojunction back contact si solar cells, IEEE J. Photovoltaics 4 (2014) 1491–1495, https://doi.org/10.1109/jphotov.2014.2358377.

[15] D. Lachenal, P. Papet, B. Legradic, R. Kramer, T. Kössler, L. Andreetta, N. Holm, W. Frammelsberger, D.L. Baetzner, B. Strahm, L.-L. Senaud, J.W. Schüttauf, A. Descœudres, G. Christmann, S. Nicolay, M. Despeisse, B. Paviet-Salomon, C. Ballif, Optimization of tunnel-junction IBC solar cells based on a series resistance model, Sol. Energy Mater. Sol. Cells 200 (2019), https://doi.org/10.1016/j.solmat.2019.110036, 110036.

[16] M.A. Green, E.D. Dunlop, D.H. Levi, J. Hohl-Ebinger, M. Yoshita, A.W.Y. Ho-Baillie, Solar cell efficiency tables (version 54), Prog. Photovoltaics Res. Appl. 27 (2019) 565–575, https://doi.org/10.1002/pip.3171.

[17] J.I. Pankove, M.L. Tarng, Amorphous silicon as a passivant for crystalline silicon, Appl. Phys. Lett. 34 (1979) 156–157, https://doi.org/10.1063/1.90711.

[18] S. De Wolf, C. Ballif, M. Kondo, Kinetics of a-si:H bulk defect and a-si:H/c-si interface-state reduction, Phys. Rev. B 85 (2012) 113302, https://doi.org/10.1103/PhysRevB.85.113302.

[19] S. Kim, V.A. Dao, Y. Lee, C. Shin, J. Park, J. Cho, J. Yi, Processed optimization for excellent interface passivation quality of amorphous/crystalline silicon solar cells, Sol. Energy Mater. Sol. Cells 117 (2013) 174–177, https://doi.org/10.1016/j.solmat.2013.05.042.

[20] T. Ruan, M. Qu, J. Wang, Y. He, X. Xu, C. Yu, Y. Zhang, H. Yan, Effect of deposition temperature of a-si:H layer on the performance of silicon heterojunction solar cell, J. Mater. Sci. Mater. Electron. 30 (2019) 13330–13335, https://doi.org/10.1007/s10854-019-01700-7.

[21] A. Descœudres, L. Barraud, S. De Wolf, B. Strahm, D. Lachenal, C. Guérin, Z. C. Holman, F. Zicarelli, B. Demaurex, J. Seif, J. Holovsky, C. Ballif, Improved amorphous/crystalline silicon interface passivation by hydrogen plasma treatment, Appl. Phys. Lett. 99 (2011), https://doi.org/10.1063/1.3641899, 123506.

[22] R. Gogolin, R. Ferré, M. Turcu, N.P. Harder, Silicon heterojunction solar cells: influence of h2-dilution on cell performance, Sol. Energy Mater. Sol. Cells 106 (2012) 47–50, https://doi.org/10.1016/j.solmat.2012.06.001.

[23] M. Mews, T.F. Schulze, N. Mingirulli, L. Korte, Hydrogen plasma treatments for passivation of amorphous-crystalline silicon-heterojunctions on surfaces promoting epitaxy, Appl. Phys. Lett. 102 (2013), https://doi.org/10.1063/1.4798292, 122106.

[24] A. Fontcuberta i Morral, P. Roca i Cabarrocas, Etching and hydrogen diffusion mechanisms during a hydrogen plasma treatment of silicon thin films, J. Non-Cryst. Solids 299–302 (2002) 196–200, https://doi.org/10.1016/s0022-3093(01)01001-8.

[25] S.N. Granata, T. Bearda, F. Dross, I. Gordon, J. Poortmans, R. Mertens, Effect of an in-situ h2 plasma pretreatment on the minority carrier lifetime of a-si:H(i) passivated crystalline silicon, in: Proceedings of the 2nd International Conference on Crystalline Silicon Photovoltaics, SiliconPV, Leuven, Belgium, 2012, pp. 412–418, https://doi.org/10.1016/j.egypro.2012.07.086, 2012.

[26] S. De Wolf, S. Olibet, C. Ballif, Stretched-exponential a-si:H/c-si interface recombination decay, Appl. Phys. Lett. 93 (2008), https://doi.org/10.1063/1.2956668.

[27] J.W.A. Schüttauf, C.H.M. van der Werf, W.G.J.H.M. van Sark, J.K. Rath, R.E. I. Schropp, Comparison of surface passivation of crystalline silicon by a-si:H with and without atomic hydrogen treatment using hot-wire chemical vapor deposition, Thin Solid Films 519 (2011) 4476–4478, https://doi.org/10.1016/j.tsf.2011.01.319.

[28] T.F. Schulze, H.N. Beushausen, C. Leendertz, A. Dobrich, B. Rech, L. Korte, Interplay of amorphous silicon disorder and hydrogen content with interface defects in amorphous/crystalline silicon heterojunctions, Appl. Phys. Lett. 96 (2010), https://doi.org/10.1063/1.3455900, 252102.

[29] H. Sai, P.-W. Chen, H.-J. Hsu, T. Matsui, S. Nunomura, K. Matsubara, Impact of intrinsic amorphous silicon bilayers in silicon heterojunction solar cells, J. Appl. Phys. 124 (2018), https://doi.org/10.1063/1.5045155.

[30] K. Ding, U. Aeberhard, F. Finger, U. Rau, Optimized amorphous silicon oxide buffer layers for silicon heterojunction solar cells with microcrystalline silicon oxide contact layers, J. Appl. Phys. 113 (2013), https://doi.org/10.1063/1.4798603, 134501.

[31] M. Boccard, Z.C. Holman, Amorphous silicon carbide passivating layers for crystalline-silicon-based heterojunction solar cells, J. Appl. Phys. 118 (2015), 065704, https://doi.org/10.1063/1.4928203.

[32] W. Liu, L. Zhang, R. Chen, F. Meng, W. Guo, J. Bao, Z. Liu, Underdense a-si:H film capped by a dense film as the passivation layer of a silicon heterojunction solar cell, J. Appl. Phys. 120 (2016), https://doi.org/10.1063/1.4966941, 175301.

[33] Y. Zhang, C. Yu, M. Yang, L. Zhang, Y. He, J. Zhang, X. Xu, Y. Zhang, X. Song, H. Yan, Significant improvement of passivation performance by two-step preparation of amorphous silicon passivation layers in silicon heterojunction solar cells, Chin. Phys. Lett. 34 (2017), https://doi.org/10.1088/0256-307x/34/3/038101.

[34] A. Descœudres, L. Barraud, R. Bartlome, G. Choong, S. De Wolf, F. Zicarelli, C. Ballif, The silane depletion fraction as an indicator for the amorphous/crystalline silicon interface passivation quality, Appl. Phys. Lett. 97 (2010) 183505, https://doi.org/10.1063/1.3511737.

[35] H. Fujiwara, M. Kondo, Impact of epitaxial growth at the heterointerface of a-si:H/c-si solar cells, Appl. Phys. Lett. 90 (2007), 013503, https://doi.org/10.1063/1.2426900.

[36] J. Yang, B. Yan, G. Yue, S. Guha, Light trapping in hydrogenated amorphous and nano-crystalline silicon thin film solar cells, MRS Proceedings 1153 (2009), https://doi.org/10.1557/PROC-1153-A13-02, 1153-A1113-1102.

[37] H. Fujiwara, M. Kondo, Effects of carrier concentration on the dielectric function of zno:Ga andin2o3:Snstudied by spectroscopic ellipsometry: analysis of free-carrier and band-edge absorption, Phys. Rev. B 71 (2005), https://doi.org/10.1103/PhysRevB.71.075109.

[38] J.C. Knights, G.L. Lucovsky, R.J. Nemanich, Defects in plasma-deposited a-si:H, J. Non-Cryst. Solids 32 (1979) 393–403, https://doi.org/10.1016/0022-3093(79)90084-X.

[39] A.A. Langford, M.L. Fleet, B.P. Nelson, W.A. Lanford, N. Maley, Infrared absorption strength and hydrogen content of hydrogenated amorphous silicon, Phys. Rev. B 45 (1992) 13367–13377, https://doi.org/10.1103/PhysRevB.45.13367.

[40] H.P. Wagner, W. Beyer, Reinterpretation of the silicon-hydrogen stretch frequencies in amorphous silicon, Solid State Commun. 48 (1983) 585–587, https://doi.org/10.1016/0038-1098(83)90520-3.

[41] A.H.M. Smets, W.M.M. Kessels, M.C.M. van de Sanden, Vacancies and voids in hydrogenated amorphous silicon, Appl. Phys. Lett. 82 (2003) 1547–1549, https://doi.org/10.1063/1.1559657.

[42] D. Reaux, J. Alvarez, M.-E. Gueunier-Farret, J.-P. Kleider, Impact of defect-pool model parameters on the lifetime in c-si/a-si:H heterojunction solar cells, Energy Procedia 77 (2015) 153–158, https://doi.org/10.1016/j.egypro.2015.07.023.

[43] A. Richter, S.W. Glunz, F. Werner, J. Schmidt, A. Cuevas, Improved quantitative description of auger recombination in crystalline silicon, Phys. Rev. B 86 (2012), https://doi.org/10.1103/PhysRevB.86.165202, 165202.

[44] C. Yu, M. Yang, G. Dong, F. Peng, D.-C. Hu, W. Long, C. Hong, G. Cui, J. Wang, Y. He, H. Yan, J. Zhang, Y. Li, X. Xu, Development of silicon heterojunction solar cell technology for manufacturing, Jpn. J. Appl. Phys. 57 (2018), 08RB15, https://doi.org/10.7567/JJAP.57.08RB15.

[45] K.-S. Lee, C.B. Yeon, S.J. Yun, K.H. Jung, J.W. Lim, Improved surface passivation using dual-layered a-SiH for silicon heterojunction solar cells, ECS Solid State Letters 3 (2014) 33–36. https://iopscience.iop.org/article/10.1149/2.001404ssl.

[46] A.B. Morales-Vilches, * E.C. Wang, T. Henschel, M. Kubicki, A. Cruz, S. Janke, L. Korte, R. Schlatmann, B. Stannowski, Improved surface passivation by wet texturing, ozone-based cleaning, and plasma-enhanced chemical vapor deposition processes for high-efficiency silicon heterojunction solar cells, Phys. Status Solidi A 217 (2020), https://doi.org/10.1002/pssa.201900518, 1900518.

[47] A.A. Langford, M.L. Fleet, B.P. Nelson, et al., Infrared-absorption strength and hydrogen content of hydrogenated amorphous-silicon, Phys. Rev. B 45 (1992) 13367–13377, https://doi.org/10.1103/PhysRevB.45.13367.

[48] S.H. Kim, V.A. Dao, C.H. Shin, J.H. Cho, Y.S. Lee, N. Balaji, S.H. Ahn, Y.K. Kim, J. Yi, Low defect interface study of intrinsic layer for c-Si surface passivation in a-Si:H/c-Si heterojunction solar cells, Thin Solid Films 521 (2012) 45–49, https://doi.org/10.1016/j.tsf.2012.03.074.

[49] L. Zhao, H.W. Diao, X.B. Zeng, C.l. Zhou, H.L. Li, W.J. Wang, Comparative study of the surface passivation on crystalline silicon by silicon thin films with different structures, Physica B 405 (2010) 61–64, https://doi.org/10.1016/j.physb.2009.08.024.

[50] T.F. Schulze, * L. Korte, F. Ruske, B. Rech, Band lineup in amorphous/crystalline silicon heterojunctions and the impact of hydrogen microstructure and topological disorder, Phys. Rev. B 83 (2011) 165314, https://doi.org/10.1103/PhysRevB.83.165314.